 https://doi.org/10.24191/jeesr.v27i1.003

Characterization of Fe-doped ZnO from Kaffir Lime Extracts for Antibacterial Applications

Muhammad Asyraf Al-Wafiy Lauthfi, Mohd Zaki Mohd Yusoff*, Suraya Ahmad Kamil, Sharifah Aminah Syed Mohamad and Nur Ubaidah Saidin

***Abstract*—In this work, ZnO nanoparticles were doped with ferrum metal to improve their ability to interact more with the bacteria. The process to fabricate ZnO is called the biosynthesis method, using lime extract to grow the ZnO nanoparticles. After the chemical process was completed, the surface morphology, and structural properties of the sample was evaluated by FESEM, EDS, and XRD measurements. XRD measurement shows a good crystalline quality of Fe-doped ZnO nanoparticles. EDS measurement is confirmed the existence of Zn, O, Fe elements in the sample. We investigated the antibacterial activity of Fe-doped ZnO NP samples at 1 mg/ml against E. coli and S. aureus. The result from the antibacterial activity of Fe-doped ZnO NP samples at 1 mg/ml against S. aureus shows that there was a 10 ± 0.6 mm inhibition zone for the mixed Fe-doped ZnO and 10% DMSO, indicating moderate activity.**

***Index Terms*— Antibacterial, citrus lime extracts, ferrum, ZnO.**

I. INTRODUCTION

Zinc oxide (ZnO) is one of the popular semiconducting materials to be used in various industrial applications. Basically, ZnO has a hexagonal wurtzite structure, and it is extensively used in the nanotechnology fields. At room temperature, the bandgap of ZnO is reported as 3.3 eV, the exciton binding energy as 60 meV, and its use in electronics and healthcare applications. ZnO nanoparticles are very useful for many optoelectronic, healthcare, and industrial fields. ZnO also offers the transparency of visible light and improves the conductivity of oscillation. It also has the potential to be applied in fabricating solar energy due to its ability to counter the optical and chemical corrosion [1, 2].

ZnO has many potentials to be used in many applications in our daily activities. ZnO has the ability to treat bacteria. Many reports used ZnO nanoparticles for the wastewater treatment [3], photocatalysis [4], and antibacterial treatment [5]. ZnO is proven to degrade the dye contamination and antibacterial applications. There are many methods that can be employed to produce ZnO nanoparticles, such as chemical deposition [6], physical sputtering [7], hydrothermal method [8], sol-gel [9], vapour deposition method [10], combustion [11], and co-precipitation [12]. One of the significant advantages of ZnO over titanium dioxide is its ability to absorb a large visible spectrum while constantly maintaining its energy band gap and also the degradation of the photocatalysis mechanism. By introducing noble metals such as titanium, silver, iron, etc. [13], ZnO is believed to expand its absorption capability and efficiency. The addition process of ions is required to reduce the energy band gap under visible light exposure for the photocatalytic process. The red shift is observed in the ZnO structure after doping with metals and nonmetals when the photocatalytic process starts [14]. Moreover, the lowered energy gap of ZnO due to the doping process helps to boost the photocatalytic process when charge separation between electron and hole increases [15, 16, 17, 18] and a new level of trap for electron and hole is created [19].

The author(s) in [20] used a two-step anodisation method to produce Fe-doped ZnO nanoparticles for photocatalytic and antibacterial applications [20]. They showed that Fe-doped ZnO nanoparticles can improve the electrical conductivity at room temperature, photocatalytic degradation, and antibacterial mechanisms [20]. The author(s) in [21] synthesised Fe-doped ZnO nanoparticles with different Fe amounts and changed their composition by introducing them to 3-aminopropyltriethoxysilane (APTES) and poly(ethylene glycol)−600 (PEG-600) [21]. High effect of antibacterial activity when using the modified Fe-doped ZnO nanoparticles under UV light exposure [21]. The author(s) in [22] used a natural extract of Myrtus communis L. to produce Fe-doped ZnO [22].

The doped ZnO showed excellent photocatalytic activity in the degradation of Acid Yellow-3 under UV light illumination [22]. Roguai and Djelloul (2021) prepared Fe-doped ZnO using a simple coprecipitation method [23], showing that the increase of Fe compositions reduced its energy gap and formed a single-phase structure [23]. Comparing all these methods, the co-precipitation method is a popular method and widely used for this material due to its low cost and ease of controlling the stoichiometry and homogeneity. The nature characteristics of ZnO nanoparticles can be altered by doping with different impurity atoms.

However, there are limited reports on ZnO nanoparticles synthesized via the biosynthesis process and doped with the ferrum element using a chemical process. Fe-doped ZnO nanoparticles used for antibacterial treatment are also reported

This manuscript is submitted on 28th May 2025, revised on 3rd June 2025, accepted on 23rd September 2025 and published on 31 October 2025.

M.A.A.W. Lauthfi, M.Z.M. Yusoff, S.A. Kamil and S.A.S. Mohamad is with Faculty of Applied Sciences, Universiti Teknologi MARA, 40450 Shah Alam, Malaysia (e-mail: asyrafwafi00@gmail.com, zaki7231@uitm.edu.my,suraya_ak@uitm.edu.my,sharifah459@uitm.edu.my).

N.U. Saidin is with Industrial Technology, Malaysian Nuclear Agency, 43000, Kajang, Selangor Malaysia (e-mail: ubaidahsaidin@gmail.com).

*Corresponding author
Email address: zaki7231@uitm.edu.my

here for the first time, as far as our knowledge is concerned. The low-cost methods are for both processes, offering a better way to reduce the chemical risk and pollution, but they are also very efficient ways to eliminate Escherichia coli (E. coli) and Staphylococcus aureus (S. aureus) bacteria.

The main objective of this work is to study the effectiveness of Fe-doped ZnO nanoparticles against Escherichia coli (E. coli) and Staphylococcus aureus (S. aureus) bacteria, respectively. The surface morphological, elemental composition, and structural characteristics were investigated by FESEM, EDX, and XRD equipment.

II. Experimental Procedure

Kaffir lime, or citrus hystrix, was used in the biosynthesis of zinc oxide nanoparticles because it was easily found in the nearby market and exhibited excellent behaviour as a bio-reduction in the treatment. The fresh kaffir lime fruits were rinsed with deionised water, and they were dried at room temperature. The juice from the fruits was manually extracted and filtered using a muslin cloth to remove unnecessary particles. 50 mL of deionised water was mixed with 0.1 M zinc acetate dihydrate, and the mixture was stirred continuously for one hour using a magnetic stirrer. 25 mL of the filtered juice was added to the mixture, followed by titration with NaOH until the pH reached 12. The mixture was continuously stirred at 500 rpm for the next three hours. One can see that the final colour of the ZnO NPs sample is brownish yellow, indicating the completion of ZnO NPs using citrus hystrix extracts. For the doping process, 0.029 g $FeCl_3$ and 1 g of ZnO were mixed in 100 ml DI water, and it was stirred for 30 minutes, as shown in Fig. 1.

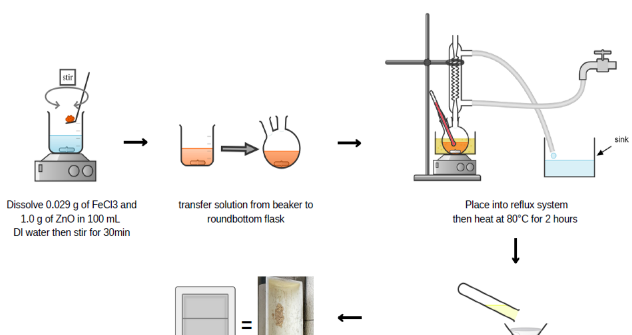

Fig. 1. A schematic diagram for the synthesis of Fe-doped ZnO NPs.

The mixture was then transferred to a round-bottom flask and heated in the reflux system at 80°C for 2 hours. The precipitates were filtered and rinsed with DI water to remove unnecessary particles. The samples were transferred to a furnace and dried at 80°C for four hours and calcined at 400°C for one hour. For the antibacterial test, the disc diffusion method using Muller-Hinton agar was used. The bacterial strains of Escherichia coli and Staphylococcus aureus were used for the antibacterial test.

Field emission scanning electron microscopy (FESEM) was used to study the surface morphology of the sample. The elemental composition of a sample was investigated by energy-dispersive X-ray (EDX) spectroscopy. The structural characteristic of a sample was examined by X-ray diffraction (XRD) machine.

III. Result And Discussion

Fig. 2 shows the FESEM image of the Fe-doped ZnO nanoparticles produced by a sol-gel method. The FESEM micrograph reveals that the Fe-doped ZnO possesses a highly agglomerated morphology constituted by nearly spherical nanoparticles, which are arranged into cauliflower-like agglomerates. The particles are uneven in size with smaller primary nanoparticles forming larger secondary particles, resulting in a porous surface texture. This morphology is largely attributed to the incorporation of Fe ions into the ZnO lattice, which interferes with the preferential c-axis growth of ZnO crystals and promotes isotropic nucleation over anisotropic rod- or wire-like morphology. So, although the particles remain within a nanoscale range, they tend to agglomerate owing to their high surface energy, as is common with oxide nanoparticles synthesized via sol-gel or precipitation pathways. Overall, the spherical, porous, and aggregated morphology of the nanoparticles is a result of the synergy between Fe doping, synthesis route, and surface energy minimization, all of which suppress the formation of well-faceted ZnO crystals.

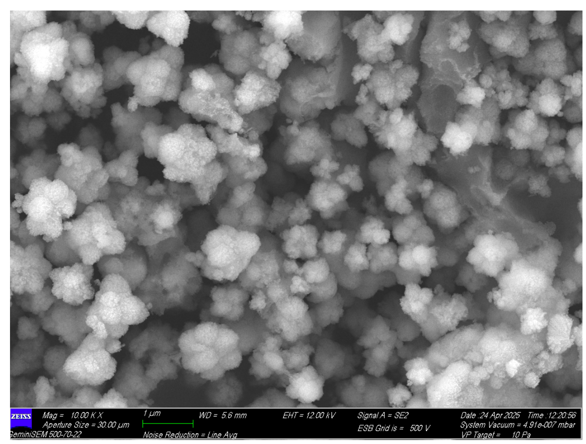

Fig. 2. FESEM image of Fe-doped ZnO NPs.

Fig. 3 indicates the EDS elemental mapping images of Fe-doped ZnO and weight elemental studies of the sample, indicating that Zn, O, and Fe are the major elements of the sample. The results confirm that there are no impurities existed and all elements were uniformly distributed on the surface of the sample, which is in good agreement EDX measurement in Fig. 4 and the FESEM image.

Fig. 5 shows the structural XRD analysis of the Fe-doped ZnO nanoparticles. The emergent peaks detected in the range spectrum between 25 and 80° were verified by the standard JCPDS card 01-074-0534 [24]. The ZnO peaks appeared at 31.85°, 34.49°, 36.33°, 47.75°, 56.66°, 63.03°, 66.73°, 68.11 and 69.29°are of respective [100], [002], [101], [102], [110], [103], [200], [112], and [201] planes. All the peaks are sharp, proving the sample has a good crystalline quality [25] and tiny size particles for the broadness at the peak bases [26]. No other elements or contamination peaks are detected, indicating a purely Fe-doped ZnO nanoparticles were successfully synthesized through this work.

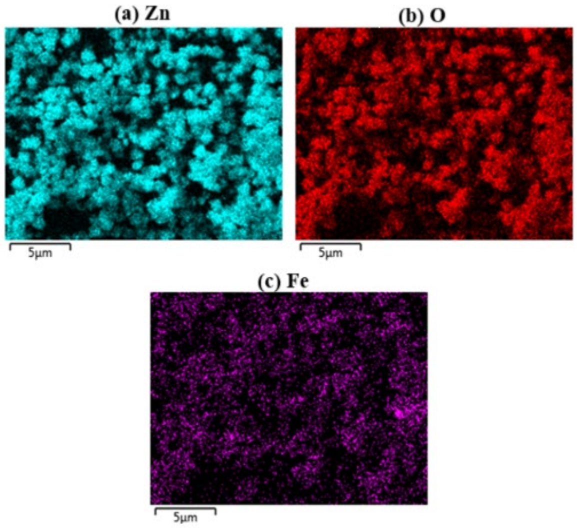

Fig. 3. EDS elemental mapping image of Fe-doped ZnO NPs. (a) Zn mapping, (b) O mapping, and (c)Fe mapping.

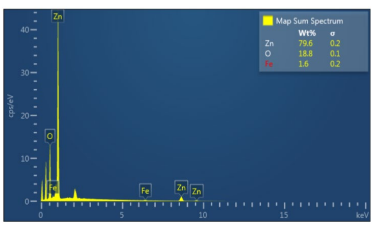

Fig. 4. EDX percent of Fe-doped ZnO NPs.

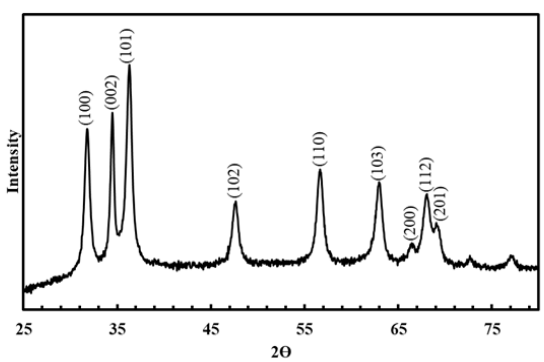

Fig. 5. A schematic diagram for the synthesis of Fe-doped ZnO NPs.

The crystallite size(s) of the ZnO nanoparticles are determined by a Debye-Scherrer formula, as in (1).

$$D = \frac{0.9\lambda}{(\beta cos\theta)} \tag{1}$$

where β is the full width at half maximum (FWHM, in radians) of the diffraction peak, Θ is the Bragg diffraction angle (in radians), D is the crystallite size (in nanometres), and λ is the x-ray wavelength (0.15406 nm).

The diffraction peak position (2Θ), full width at half maximum (FWHM), and crystallite size were presented in Table 1. The average crystallite size is calculated as 10.50 nm, confirming that the ZnO is in the nano size range.

TABLE I CRYSTALLITE SIZE OF ZNO NPS AT DIFFERENT DIFFRACTION PEAK POSITION

2Θ	FWHM	Crystallite Size (nm)
31.79924	0.63917	13.5
34.48278	0.4856	17.89
36.28464	0.61727	14.15
47.61667	1.26485	7.17
56.65802	0.98506	9.57
62.94316	1.2086	8.05
68.19423	3.12905	3.2

The effectiveness of doped ZnO of antibacterial reaction depends on several factors such as physico-chemical, type and concentration of ion dopant, dye structure, and bacterial type [27]. Table 2 shows the antibacterial activity of Fe-doped ZnO NPs samples at 1 mg/ml against E. coli. We found that the Fe-doped ZnO in 10% DMSO solution showed significant antibacterial activity with a mean inhibition zone of 21 ± 0.6 mm. However, when the Fe-doped ZnO NPs samples were mixed with 10% methanol solution, there was no activity observed. Meanwhile, Fe-doped ZnO was mixed with 10% acetic acid, and a 10 ± 0.6 mm inhibition zone was created, showing a moderate reaction. On the other hand, positive control of ciprofloxacin shows a significant antibacterial reaction with an inhibition zone of 38 mm. While for the negative control samples, there is no activity detectable except for the 10 % acetic acid solution.

TABLE 2. ANTIBACTERIAL ACTIVITY OF NANOPARTICLE SAMPLES AT 1 MG/ML AGAINST E.COLI

Solvent	Inhibition Zone (mm)			
	1	2	3	Mean ± SD
10% DMSO	21	21	20	21 ± 0.6
10% Methanol	NA	NA	NA	NA
10% Acetic Acid	11	10	10	10±0.6
PC, 1 mg/ml ciprofloxacin	38	-	-	-
NC, 10% DMSO	NA	-	-	-
NC, 10% Methanol	NA	-	-	-
NC, 10% Acetic Acid	20	-	-	-

Table 3 shows the antibacterial activity of Fe-doped ZnO NPs samples at 1 mg/ml against S. aureus. We observed that there was a 10 ± 0.6 mm inhibition zone for the mixed Fe-doped ZnO and 10% DMSO, showing moderate activity. When the Fe-doped ZnO was mixed with 10% methanol, the mean inhibition zone was recorded as 16 ± 1.2 mm, indicating good antibacterial activity.

TABLE 3. ANTIBACTERIAL ACTIVITY OF NANOPARTICLE SAMPLES AT 1 MG/ML AGAINST *S. AUREUS*

Solvent	Inhibition Zone (mm)			
	1	2	3	Mean ± SD
10% DMSO	10	9	10	10 ± 0.6
10% Methanol	16	16	18	16 ±1.2
10% Acetic Acid	12	12	13	12±0.6
PC, 1 mg/ml ciprofloxacin	25	-	-	-
NC, 10% DMSO	NA	-	-	-
NC, 10% Methanol	NA	-	-	-
NC, 10% Acetic Acid	17	-	-	-

Moderative reaction is also reported when Fe-doped ZnO was placed in 10% acetic acid, generating a 12 ± 0.6 mm inhibition zone. Besides, positive control (ciprofloxacin) shows an inhibition zone of 25 mm, which is a higher antibacterial activity rate. While there was no activity observed for the negative control (10% DMSO and 10% methanol), except for 10% acetic acid, with an inhibition zone of 17 mm. Previous work states that the antibacterial activity increased when applying to both gram-negative and positive bacterial species, compared without doping [27]. Besides, same finding also discovered from previous works [28-30], when they investigated the impact of different metals doping on the antibacterial mechanism of ZnO nanoparticles.

The author(s) in [31] reported that the Fe-doped ZnO NPs with Fe 5wt% content showed the highest efficacy of bacterial inhibition for E. Coli [31]. Previous work has indicated the Fe 5wt% content improved the bacterial inhibition, where Zn^{2+} ion was released from the process of reactive oxygen species (ROS) to interrupt cellular functions and form defect [32]. Meanwhile, lower Fe content in ZnO indicates a higher antimicrobial activity compared with the undoped ZnO NPs.

There were several factors that may influence the effectiveness of the doping compound on the photocatalytic and antimicrobial activities, such as physico-chemical properties of nanomaterials, the type and concentration of dopant, and the dye and bacterial cell's structure [32]. Moreover, the decreasing particle size of ZnO will increase the antimicrobial activity, where the surface-to-volume ratio has increased, resulting more efficiency for antibacterial activity [33]. The concentration of particle medium is also reported to be more effective in growing a larger bacterial inhibition area than particle size [34]. Meanwhile, other works reported a ZnO has a better antibacterial result for Gram-positive bacteria than Gram-negative bacteria [34]. The structure of the cell membrane is the cause of the different results of both Gram-positive and negative bacteria. Gram-positive bacteria are characterized by peptidoglycan layer, teichoic, and lipoteichoic acids. While Gram-negative bacteria are formed by lipopolysaccharide and peptidoglycan materials, which protect it from the damage caused by the ZnO particles. Overall, Fe-doped ZnO nanoparticles are beneficial in treating both Gram-positive and Gram-negative samples. These findings were well in agreement with other reports [34, 35], where ZnO nanoparticles have been proven to perform the antibacterial activity.

IV. CONCLUSION

As a conclusion, we have successfully synthesized Fe-doped ZnO nanoparticles using kaffir lime extracts for antibacterial applications. FESEM result shows the spherical agglomeration of Fe-doped ZnO nanoparticles. EDS measurement confirms the presence of all important elements in the doped material. XRD analysis indicates a good crystalline quality of the sample. For the antibacterial activity of Fe-doped ZnO NP samples at 1 mg/ml against E. coli. The Fe-doped ZnO in a 10% DMSO solution indicated important antibacterial activity with a mean inhibition zone of 21 ± 0.6 mm. The result from the antibacterial activity of Fe-doped ZnO NP samples at 1 mg/ml against S. aureus shows that there was a 10 ± 0.6 mm inhibition zone for the mixed Fe-doped ZnO and 10% DMSO, indicating moderate activity.

ACKNOWLEDGMENT

This study was funded by the Ministry of Higher Education Malaysia through the Fundamental Research Grant Scheme (FRGS) with code FRGS/1/2023/STG05/UITM/02/6. The support from Universiti Teknologi Mara, Shah Alam, is also gratefully acknowledged.

REFERENCES

[1] C. Cruz-Vázquez, R. Bernal, S. E. Burruel-Ibarra, H. Grijalva-Monteverde, and M. Barboza-Flores, "Thermoluminescence properties of new ZnO nanophosphors exposed to beta irradiation," *Opt. Mater.*, vol. 27, no. 7, pp. 1235–1239, 2005.

[2] P. Kumbhakar, D. Singh, C. S. Tiwary, and A. K. Mitra, "Chemical synthesis and visible photoluminescence emission from monodispersed ZnO nanoparticles," *Chalcogenide Lett.*, vol. 5, no. 12, pp. 387–394, 2008.

[3] M. Aliannezhadi, F. Doost Mohamadi, M. Jamali, and F. Shariatmadar Tehrani, "Ultrasound-assisted green synthesized ZnO nanoparticles with different solution pH for water treatment," *Sci. Rep.*, vol. 15, no. 1, pp. 7203, 2025.

[4] N. T. T. Nguyen, A. N. Q. Phan, T. Van Tran, and T. T. T. Nguyen, "Morinda citrifolia fruit extract-mediated synthesis of ZnO and Ag/ZnO nanoparticles for photocatalytic degradation of tetracycline," *Environ. Res.*, vol. 273, pp. 121209, 2025.

[5] H. Zhang *et al.*, "Low-temperature one-step synthesis of cerium doped ZnO nanoparticles for antibacterial application," *Chem. Eng. Sci.*, vol. 311, pp. 121628, 2025.

[6] R. Nasrin, M. O. Haq, and M. A. Rahman, "Influence of metal doping on topographic, microstructural, optical and thermal properties of zinc oxide nanoparticles," *Appl. Phys. A*, vol. 130, no. 7, pp. 473, 2024.

[7] P. Kaim *et al.*, "The influence of magnetron sputtering process temperature on ZnO thin-film properties," *Coatings*, vol. 11, no. 12, pp. 1507, 2021.

[8] M. M. ElFaham, A. M. Mostafa, and E. A. Mwafy, "The effect of reaction temperature on structural, optical and electrical properties of tunable ZnO nanoparticles synthesized by hydrothermal method," *J. Phys. Chem. Solids*, vol. 154, pp. 110089, 2021.

[9] S. Arya *et al.*, "Influence of processing parameters to control morphology and optical properties of Sol-Gel synthesized ZnO nanoparticles," *ECS J. Solid State Sci. Technol.*, vol. 10, no. 2, pp. 023002, 2021.

[10] S. Park *et al.*, "Production of an EP/PDMS/SA/AlZnO coated superhydrophobic surface through an aerosol-assisted chemical vapor deposition process," *Langmuir*, vol. 38, no. 25, pp. 7825–7832, 2022.

[11] N. Sharma and P. P. Sahay, "Solution combustion synthesis of Dy-doped ZnO nanoparticles: An investigation of their structural, optical and photoluminescence characteristics," *J. Lumin.*, vol. 257, pp. 119655, 2023.

[12] S. Ghosh *et al.*, "Synthesis of ZnO nanoparticles by co-precipitation technique and characterize the structural and optical properties of these

nanoparticles," in *J. Phys.: Conf. Ser.*, vol. 2349, no. 1, p. 012014, Sep. 2022.

[13] Z. Wang *et al.*, "Progress on extending the light absorption spectra of photocatalysts," *Phys. Chem. Chem. Phys.*, vol. 16, no. 7, pp. 2758–2774, 2014.

[14] S. G. Kumar and K. K. Rao, "Zinc oxide based photocatalysis: tailoring surface-bulk structure and related interfacial charge carrier dynamics for better environmental applications," *RSC Adv.*, vol. 5, no. 5, pp. 3306–3351, 2015.

[15] R. Chauhan, A. Kumar, and R. P. Chaudhary, "Photocatalytic studies of silver doped ZnO nanoparticles synthesized by chemical precipitation method," *J. Sol-Gel Sci. Technol.*, vol. 63, pp. 546–553, 2012.

[16] R. Saleh and N. F. Djaja, "Transition-metal-doped ZnO nanoparticles: synthesis, characterization and photocatalytic activity under UV light," *Spectrochim. Acta A Mol. Biomol. Spectrosc.*, vol. 130, pp. 581–590, 2014.

[17] C. C. Piras, S. Fernández-Prieto, and W. M. De Borggraeve, "Ball milling: a green technology for the preparation and functionalisation of nanocellulose derivatives," *Nanoscale Adv.*, vol. 1, no. 3, pp. 937–947, 2019.

[18] A. Hui, J. Ma, J. Liu, Y. Bao, and J. Zhang, "Morphological evolution of Fe doped sea urchin-shaped ZnO nanoparticles with enhanced photocatalytic activity," *J. Alloys Compd.*, vol. 696, pp. 639–647, 2017.

[19] D. Wang, H. Noguchi, T. Kako, and J. Ye, "Photocatalytic activity of silver-loaded or unloaded titanium dioxide coating in the removal of hydrogen sulfide," *Res. Chem. Intermed.*, vol. 31, no. 4, pp. 441–448, 2005.

[20] J. A. Joseph *et al.*, "Zinc-doped iron oxide nanostructures for enhanced photocatalytic and antimicrobial applications," *J. Appl. Electrochem.*, vol. 51, pp. 521–538, 2021.

[21] X. Sun, J. Yu, X. Li, H. Chen, and Y. Gao, "Synthesis, characterization and antibacterial mechanism study of small water-soluble iron-doped zinc oxide nanoparticles," *Colloids Surf. A Physicochem. Eng. Asp.*, vol. 686, pp. 133421, 2024.

[22] F. A. Jan, R. Ullah, N. Ullah, and M. Usman, "Exploring the environmental and potential therapeutic applications of Myrtus communis L. assisted synthesized zinc oxide (ZnO) and iron doped zinc oxide (Fe-ZnO) nanoparticles," *J. Saudi Chem. Soc.*, vol. 25, no. 7, pp. 101278, 2021.

[23] S. Roguai and A. Djelloul, "Structural, microstructural and photocatalytic degradation of methylene blue of zinc oxide and Fe-doped ZnO nanoparticles prepared by simple coprecipitation method," *Solid State Commun.*, vol. 334, pp. 114362, 2021.

[24] S. Kumar *et al.*, "Insight into the origin of ferromagnetism in Fe-doped ZnO diluted magnetic semiconductor nanocrystals: an EXFAS study of local structure," *RSC Adv.*, vol. 5, no. 115, pp. 94658–94669, 2015.

[25] M. C. Sekhar *et al.*, "Influence of Sm doping on the structural, optical, and magnetic properties of ZnO nanopowders," *J. Supercond. Nov. Magn.*, vol. 30, pp. 1937–1941, 2017.

[26] Y. S. Rao *et al.*, "Effect of Fe doped and capping agent–structural, optical, luminescence, and antibacterial activity of ZnO nanoparticles," *Chem. Phys. Impact*, vol. 7, pp. 100270, 2023.

[27] V. Mușat, M. Ibănescu, D. Tutunaru, and F. Potecaşu, "Fe-Doped ZnO Nanoparticles: Structural, Morphological, Antimicrobial and Photocatalytic Characterization," *Adv. Mater. Res.*, vol. 1143, pp. 233–239, 2017.

[28] M. Bușilă, V. Mușat, T. Textor, and B. Mahltig, "Synthesis and characterization of antimicrobial textile finishing based on Ag: ZnO nanoparticles/chitosan biocomposites," *RSC Adv.*, vol. 5, no. 28, pp. 21562–21571, 2015.

[29] Y. J. Lin, X. Y. Xu, L. Huang, D. G. Evans, and D. Q. Li, "Bactericidal properties of ZnO–Al_2O_3 composites formed from layered double hydroxide precursors," *J. Mater. Sci. Mater. Med.*, vol. 20, pp. 591–595, 2009.

[30] A. C. Manna, "Synthesis, characterization, and antimicrobial activity of zinc oxide nanoparticles," in *Nano-antimicrobials: Progress and Prospects*, Berlin, Germany: Springer, pp. 151–180, 2011.

[31] M. Tahir, Z. H. Shah, A. F. Butt, and M. Imran, "Antibacterial efficacy of iron-doped zinc oxide nanoparticles for the control of hospital-acquired infections," *Nature's Symphony*, vol. 3, no. 1, pp. 1–19, 2025.

[32] V. Mușat, M. Ibănescu, D. Tutunaru, and F. Potecaşu, "Fe-doped ZnO nanoparticles: Structural, morphological, antimicrobial and photocatalytic characterization," *Adv. Mater. Res.*, vol. 1143, pp. 233–239, 2017.

[33] C. Baker, A. Pradhan, L. Pakstis, D. J. Pochan, and S. I. Shah, "Synthesis and antibacterial properties of silver nanoparticles," *J. Nanosci. Nanotechnol.*, vol. 5, no. 2, pp. 244–249, 2005.

[34] Z. Emami-Karvani and P. Chehrazi, "Antibacterial activity of ZnO nanoparticle on gram-positive and gram-negative bacteria," *Afr. J. Microbiol. Res.*, vol. 5, no. 12, pp. 1368–1373, 2011.

[35] Z. Lingling, J. Yunhong, E. Ding Yulong, M. Povey, and D. York, "Investigation into the antibacterial behaviour of suspensions of ZnO nanoparticles (ZnO nanofluids)," *J. Nanopart. Res.*, vol. 9, no. 3, pp. 479–489, 2007.

.